Title	The effects of array configuration on the hydro-environmental impacts of tidal turbines.
Author(s)	Fallon, David; Nash, Stephen
Publication Date	2012
Publication Information	Fallon, D; Nash, S (2012) The effects of array configuration on the hydro-environmental impacts of tidal turbines 4th International Conference on Ocean Energy
Item record	http://hdl.handle.net/10379/3490

The Effects of Array Configuration on the Hydro-environmental Impacts of Tidal Turbines

D. Fallon[1, 2] and Dr S. Nash[1, 2]

[1]College of Engineering and Informatics, National University of Ireland, Galway.
[2]Ryan Institute for Environmental, Marine and Energy Research, National University of Ireland, Galway.
E-mail: david.fallon@nuigalway.ie and stephen.nash@nuigalway.ie

Abstract

Tidal stream turbines provide a technically viable means of generating electricity from a sustainable resource; however, economic viability will require the deployment of multiple devices in array formations in a manner analogous to wind farms. This research investigates the effect of the configuration of a tidal turbine array on the hydro-environmental impacts of the array such as changes in tidal flows and water surface levels.

The Shannon Estuary, a highly energetic estuary on the west coast of Ireland with significant potential for tidal current energy extraction, was simulated using a depth integrated 2D hydro-environmental model, namely DIVAST. The numerical model was modified to incorporate the effects of energy extraction on the tidal regime and a multiple device array was simulated. Three different array configurations were examined with turbine spacings of 0.5, 2 and 5 rotor diameters. The model results demonstrate that energy extraction has an attenuation effect on the currents within the array while flow is accelerated around the array. Water surface elevations are also affected with a reduction in tidal range upstream of the array. The magnitude and extent of the observed impacts are greater for the smallest turbine spacing but were still significant for the larger spacings.

Keywords: Array configuration, energy extraction, hydro-environmental impacts and Shannon Estuary.

1. Introduction

Presently, trial-scale and full-scale turbines have successfully connected to national grids. These turbines include SeaGen, located in Strangford Lough, Ireland and Seaflow near the North Devon coast, UK, both of which are owned and operated by Marine Current Turbines Ltd., UK [1] and the Open-Centre turbine installed in the Minas Passage, Bay of Fundy, Canada by OpenHydro Ltd., Ireland [2]. Progression from these single turbine deployments will involve installation of turbine arrays (farms). The configuration of these arrays will be site specific and there are many factors which will determine the device geometry and spacing. In addition, these arrays will alter ambient flow patterns, as there will be a reduction in flow downstream of the turbines. This retardation occurs due to the flow in the turbine's wake moving at a lower velocity than the free stream (which is diverted around the turbines); consequently the slower moving flow must expand to preserve momentum [3].

2. Hydro-environmental Model Details

The model used for this research was DIVAST (Depth Integrated Velocities and Solute Transport), a two-dimensional, depth integrated, finite difference model developed for hydrodynamic modelling of shallow, and near-shore waters in the coastal zone.

2.1 Governing equations

The model is capable of replicating the tidal regime, solute transport and water quality in reasonably shallow estuarine and coastal water bodies [4-7]. The governing differential equations employed by the model to ascertain the water surface elevations and depth integrated velocity fields in the horizontal plane are based on integrating the Navier-Stokes and continuity equations (three-dimensional) throughout the depth of the water column. The depth integrated continuity and x direction momentum equations (similarly for y-direction) can be presented in the following form [Eq. 1 and 2]:

Continuity equation:

$$\frac{\partial \zeta}{\partial t} + \frac{\partial q_x}{\partial x} + \frac{\partial q_y}{\partial y} = 0 \qquad (1)$$

X-direction momentum equation:

$$\frac{\partial q_x}{\partial t} + \beta \left[\frac{\partial U q_x}{\partial x} + \frac{\partial U q_y}{\partial y} \right] = f q_y - gH \frac{\partial \zeta}{\partial x}$$
$$+ \frac{\tau_{xw}}{\rho} - \frac{\tau_{xb}}{\rho} + 2\frac{\partial}{\partial x}\left[\varepsilon H \frac{\partial U}{\partial x} \right] +$$
$$\frac{\partial}{\partial y}\left[\varepsilon H \left[\frac{\partial U}{\partial y} + \frac{\partial V}{\partial x} \right] \right] \quad (2)$$

Where t = time (s); ζ = water surface elevation above datum (m); q_x, q_y = depth averaged volumetric flux components in the x, y directions (m^2 s^{-1}); U,V = depth averaged velocity components in the x, y directions(m s^{-1}); β = momentum correction factor (dimensionless); f = Coriolis parameter (rad s^{-1}); g = gravitational acceleration (m s^{-2}); ρ = fluid density (kg m^{-3}); τ_{xw},τ_{yw} = surface wind shear stress components in the x,y directions (N m^{-2}); τ_{xb}, τ_{yb} = bed shear stress components in the x,y directions (N m^{-2}) and ε = depth averaged eddy viscosity.

The model employs an implicit finite difference scheme based upon the Alternating Direction Implicit (ADI) technique to solve the governing differential equations. This technique divides each time step into two half-time steps, enabling a two-dimensional implicit scheme to be applied; however, only one dimension is considered implicitly for each half-time step. The major advantage with this approach is that it eradicates the requirement for solving a complete two-dimensional matrix and reduces the computational cost [8]. The model carries out computations on a uniform rectilinear grid with equivalent grid spacings in the x and y planes.

2.2 Turbine representation

Inclusion of tidal turbines in the numerical model was based on work carried out by [9] on Linear Momentum Actuator Disc Theory (LMADT). This theory considers a stream tube enclosing a turbine rotor which is modelled as an actuator disk which adds momentum and energy to the flow in an open channel. Fig. 1 illustrates five stations (1) far upstream of the turbine, (2) immediately upstream of the turbine, (3) immediately downstream of the turbine, (4) the region where the slower moving flow from the turbine's wake merges with the free stream fluid from the by-pass flow and (5) adequately far enough downstream from the turbine that the pressure regains uniformity. The section of the flow passing through the turbine (illustrated in yellow in Fig. 1) contains the subscript "t" and the by-pass flow (highlighted in red in Fig. 1) is denoted by the subscript "b".
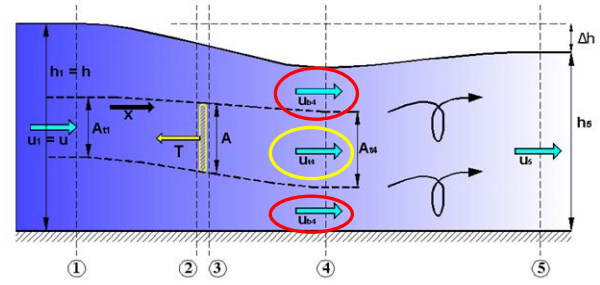

Figure 1: linear momentum disk theory in an open channel flow

The undisturbed flow at the inflow boundary (1) moves through the stream tube until it reaches the proximity of the turbine which exerts an equal and opposite thrust force (T) which complies with Newton's third law. The turbine thrust force (T) and the thrust coefficient (C_T) is expressed as;

$$T = \frac{1}{2}\rho u^2 A C_T \quad (3)$$

$$C_T = \left(\beta_4^2 - \alpha_4^2 \right) \quad (4)$$

Where T = turbine thrust force (N); ρ = fluid density (kg m^{-3}); u = velocity (m s^{-1}); A = area of turbine defined as an actuator disc (m^2) C_T = Dimensionless thrust coefficient, normalised by upstream kinetic pressure; β_4 Bypass flow velocity coefficient and α_4 = Turbine wake flow velocity coefficient.

The model incorporates this turbine thrust force as a sink term (negative term) in the momentum equation which facilitates a more accurate investigation of the effects of energy extraction. Previous research [3] confirms that the flow passing through the turbine will experience a reduction in velocity across the rotor plane (2 to 3). Immediately downstream of the turbine (3 to 4), the flow is moving at a slower velocity than the free stream fluid (that was diverted around the rotor) and therefore must expand to satisfy conservation of momentum. This action generates the turbine's wake (cone-shaped region downstream of the rotor) which also contains turbulent mixing. At a sufficient distance far downstream the wake will have almost entirely dissipated and the flow at station (5) will revert to its undisturbed state experienced far upstream (1).

The numerical model was modified to incorporate the turbines and their associated impacts by including a reaction force, namely, the axial thrust that is induced by turbines as an external force in the shallow water momentum equations [Eq. 5]. Inclusion of this momentum sink term provides a more comprehensive determination into the effects of energy extraction.

Similar studies which have incorporated the reaction of the axial thrust induced by the turbines have been carried out by [10] and [11]. Subsequently, the x-direction momentum equation (similarly for y direction) was amended as follows [Eq. 5];

$$\frac{\partial q_x}{\partial t} + \beta \left[\frac{\partial U q_x}{\partial x} + \frac{\partial U q_y}{\partial y} \right] = f q_y - gH \frac{\partial \zeta}{\partial x}$$

$$+ \frac{\tau_{xw}}{\rho} - \frac{\tau_{xb}}{\rho} + 2 \frac{\partial}{\partial x} \left[\varepsilon H \frac{\partial U}{\partial x} \right] + \qquad (5)$$

$$\frac{\partial}{\partial y} \left[\varepsilon H \left[\frac{\partial U}{\partial y} + \frac{\partial V}{\partial x} \right] \right] + \boxed{\frac{F_{Tx}}{\rho}}$$

Where F_{Tx} = is the axial thrust induced by the turbines on the flow, this force is equal and opposite, therefore, satisfying Newton's third law of motion. The total of the reaction of the axial thrust induced by the turbines on the tidal regime can be expressed as:

$$F_T = \frac{T}{\Delta x \times \Delta y} = \frac{1}{2} \times \frac{1}{\Delta x \times \Delta y} C_T \rho A U_{tot}^2 \qquad (6)$$

Where C_T = thrust coefficient (dimensionless), and for the purpose of this research a C_T value of 0.5 was selected due current advancements in turbine design and efficiency. The velocity perpendicular to the turbine or parallel to the turbine axis is known as the total flow velocity (U_{tot}). Modern turbines can be designed to be unidirectional which ensures that the flow is always acting normally to the turbine cross-sectional area, or alternatively they can rotate by 180° (bidirectional) to face the flow from the ebb and flood stages of the tide. The model used in the current research assumes that the turbine axis is always perpendicular to the flow. Assuming that the angle which the turbine axis makes with the positive y direction is θ (Fig. 2), and then each vector component of the reaction force of the axial thrust induced by the turbines on the tidal regime can be presented by:

$$F_{Tx} = F_T \times \left| \sin(\theta) \right| \times sign(u) \qquad (7)$$

$$F_{Ty} = -F_T \times \left| \cos(\theta) \right| \times sign(v) \qquad (8)$$

Where F_T, F_{Tx}, and F_{Ty} = the total, x and y vector components of the reaction force of the axial thrust reaction induced by the turbines on the flow per unit area, u and v = the x and y directions velocity components, respectively and sign(u) and sign(v) = sign convention which specifies a value of +1 when u and v makes positive with the x and y direction correspondingly and similarly a value of -1 when u and v makes negative with the x and y directions.
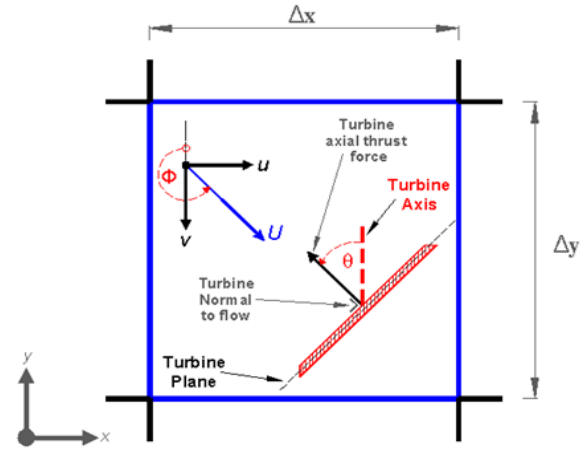

Figure 2: Schematic of turbine axial thrust force and velocity components

3. Model Application – Shannon Estuary

The Shannon Estuary is a long and narrow estuary where the River Shannon flows into the Atlantic Ocean. The estuary is approximately 87 km in length from head to mouth and has a surface area in excess of 500 km². A technical report by Sustainable Energy Ireland [12] identified the Shannon Estuary as one of eleven Irish sites deemed suitable for harnessing tidal energy. The hydrodynamic model was calibrated against measured data on tidal elevations at 6 locations (T1 – T6) and tidal stream velocities at location C1 (Fig. 3), acquired from Admiralty Charts. Spring and neap tidal amplitudes of 1.89 and 0.8 m were specified at the open boundaries respectively to correspond to ambient conditions at the time of measurement. Fig. 4 illustrates the measured data of spring and neap tidal currents against the predicted data.
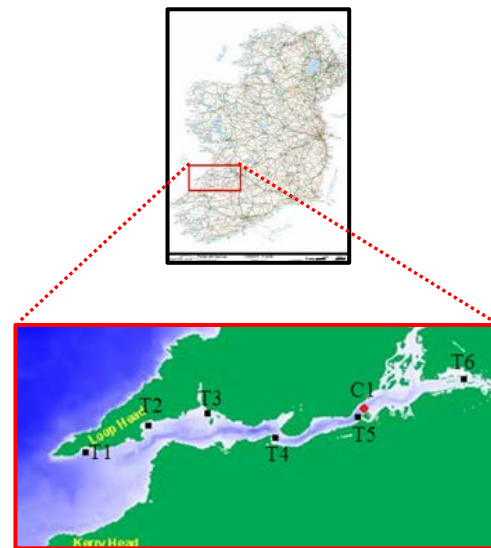

Figure 3: Locations of measured data for tidal amplitudes (T1- T6) and tidal current velocities (C1) in the Shannon Estuary
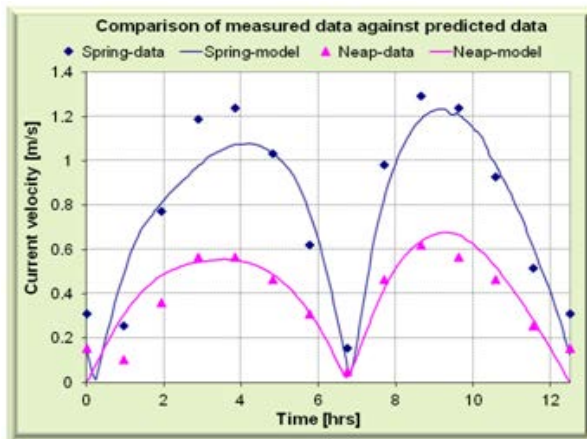
Figure 4: Comparison of measured data against the model predicted data

3.1 Model details

Bathymetry data was obtained from digitised Admiralty Charts of the Shannon Estuary. This data was then interpolated onto a finite difference grid at a spatial resolution of 189 m x 189 m. Consequently, a computational domain was created, which subsequently, generated 507 x 217 grid cells. Flow boundaries were specified upstream for both the River Shannon (east) and River Fergus (north) respectively and water elevation boundaries were set downstream on the peripheries of the domain (Fig. 5). The latter's boundary conditions were responsible for the principal forcing functions that induced water circulation within the estuary. The model simulation was executed for 37.5 h over a constant spring tidal cycle. The turbine farm domain (black dashed line) is also depicted in Fig. 5.
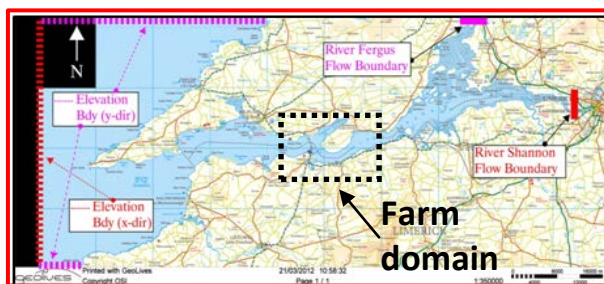

Figure 5: Shannon Estuary model domain extents including boundary locations (Courtesy of Geolives)

3.2 Model scenarios

The amended hydrodynamic model was used to simulate 3 multi-device arrays of tidal turbines for the Shannon Estuary. This study investigated the effects of these configurations on the hydro-environmental impacts of the array, such as changes in tidal flows and water surface levels. Three different array configurations were examined, having turbine spacings

of 0.5, 2 and 5 rotor diameters (centre to centre). A schematic of the lowest turbine array density (5 rotor diameters = 96 m c/c) is presented in Fig. 6. A rotor diameter of 16 m was used in this research which was based on SeaGen, Marine Current Turbines 1st commercially deployed tidal turbine [13]. Consequently, the rotor diameter stipulates a limitation on water depth within the confines of the turbine farm. As a result, turbines were only deployed where water depths greater than 20 m at low spring tide existed.
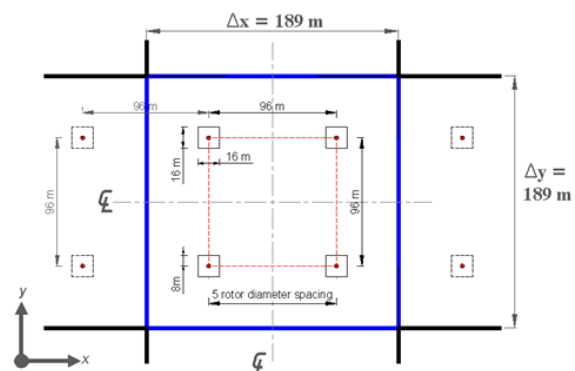

Figure 6: Schematic of turbine array at 5 rotor diameter spacings for each grid cell

The tidal turbine farm location was selected because it is the region of highest available tidal current energy resource in the estuary due to the presence of significant tidal currents. A contour plot of the turbine farm domain is presented in Fig. 7 and there are two contour bands depicted on the map. The contour depth band from 0 to 20 m is outside the turbine farm because the rotor diameter of 16 m requires the water depth to be in excess of 20 m. Location S1 is sited within the turbine farm and point S2 is outside of the farm. The current velocities at both locations were compared against to observe their interactions on the flow.
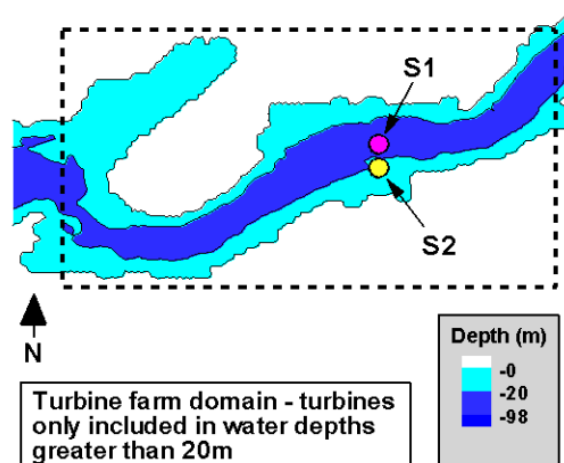

Figure 7: Model domain extents of turbine farm including site locations S1 (inside) and S2 (outside)

4. Results

Model results were analysed to determine the effects of array configurations on the hydro-environmental impacts of energy extraction. Current velocities were analysed to determine the impacts of energy extraction on tidal flows. Whereas, the water surface elevations were investigated to establish the consequences of energy harvesting on the tidal regime.

There were a total of 22 time-trace locations specified in the model at which tidal current velocities and water surface elevations were output. However, for clarity, 4 time-trace locations are examined (Fig. 8), one each upstream (U1) and downstream (D1) of the turbine farm and 2 further locations, one inside (S1) and one outside (S2) of the farm domain (Fig. 8). Location (S2) is outside the turbine farm domain (Fig. 7 and 8s 7 and 8) because the water depth at this site is less than 20 m (the minimum depth required for turbine deployment). The model was run for three tidal cycles (37.5 hrs); however, for clarity only one tidal cycle is illustrated in the results.
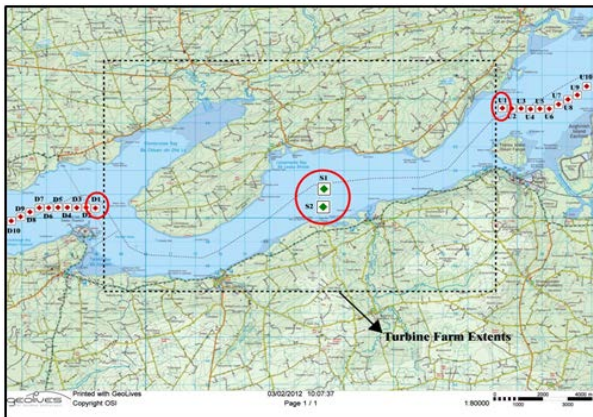

Figure 8: Map of time-trace locations at D1, S1, S2 and U1 (Courtesy of Geolives)

4.1 Tidal flows

The model was run for four different scenarios; (1) without turbines, (2) including turbines at 0.5 rotor diameter spacings, (3) including turbines at 2 rotor diameter spacings and (4) including turbines at 5 rotor diameter spacings. Fig. 9 depicts the current velocities within the turbine farm (S1) and Fig. 10 illustrates the velocities outside the farm (S2). The model results demonstrate that energy extraction has an attenuation effect on the currents within the array while flow is accelerated around the array (S2); this agrees with the findings of studies by [14] and [3]. This increase in velocity around the turbine farm is caused by 'blockage' effects, which occurs when the upper and lower extremities of a turbine is in close proximity to the water surface and the seabed [15].
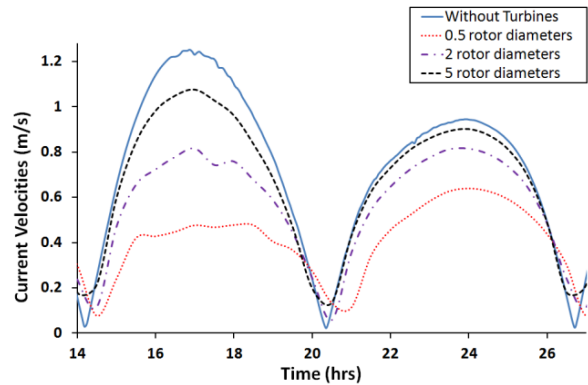

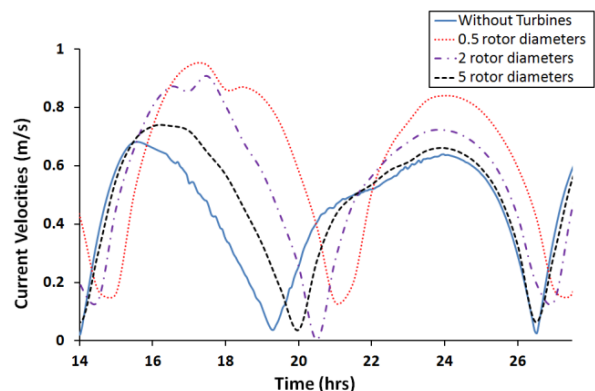**Figure 9:** Comparison of current velocities inside turbine farm (S1) for the various array configurations

Figure 10: Comparison of current velocities **outside** turbine farm (S**2**) for the various array configurations

At the highest turbine density the effects of energy extraction are observed with a substantial reduction in velocities occurring inside and outside the farm. A time lag occurs at high and low water at this configuration. The effects of current attenuation on the flood tide are more significant within the array since energy is extracted from the water by the turbines within the farm, resulting in a retardation of the current.

Outside the farm The middle density array (2 rotor diameters) produced results with less significant effects than the higher density array when energy extraction was considered, while, there is still a sizeable reduction in velocities within the farm and an acceleration of flow outside the farm. The time lag at this density reduces within the farm because the density of the turbines increased (compared to the 0.5 rotor diameter case) and therefore, there is less water backing up when engaging the turbines and the time it takes to culminate in high and low tide is not delayed as much. There were still changes in flows observed at 5 rotor diameter spacings, but they are not as significant as at 0.5 rotor diameter spacings.
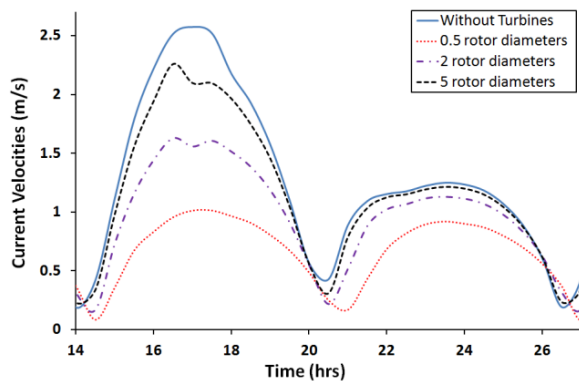
Figure 11: Comparison of current velocities downstream of turbine farm (D1) for the various array configurations
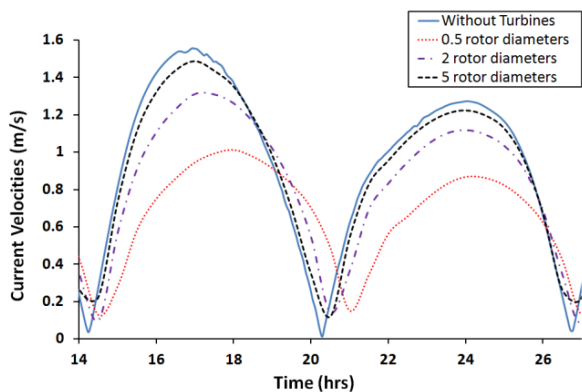

Figure 12: Comparison of current velocities upstream of turbine farm (U1) for the various array configurations

Fig. 11 and Fig. 12 compares the tidal current velocities of a spring tide for the four model scenarios at locations specified downstream of the farm (D1) and upstream of the farm (U1). At the highest array density (0.5 rotor diameter spacings) there are significant reductions in velocities when energy extraction occurs, especially on the ebb tide. A time lag also occurs at this density resulting in a delay of the times of high and low water. The effects of energy extraction on the middle array density (2 rotor diameter spacings) were similar, but, less significant to the higher density case. In addition the time lag is not as considerable at this configuration.

At the greatest turbine spacings (5 rotor diameters) energy is extracted on the flood tide as the wave propagates through the turbine farm, and therefore, less energy reaches the locations upstream (U1). We can see this affects the ebb current which has less energy at the upstream point because of the energy extraction process of the flood tide. Both the flood and ebb tides have a lower energy content that manifests itself as a reduction in kinetic energy and current velocities. Downstream (D1), the flood tide hasn't passed through the turbines and remains relatively unchanged, but on the ebb tide we can see a significant difference. The reason for this difference is that the flood tide is dominated by the open ocean at the mouth of the estuary and contains maximum energy content; in

contrast, energy has been removed as the flood tide passes through the turbines which means that there is a lower energy content available when the ebb tide process commences. This lower array density is more realistic, although there are still significant changes in the maximum current velocities and the time lag occurs once more.

4.2 Tidal regime

To evaluate the tidal regime in the Shannon Estuary, the model output consisted of water surface elevations. The water surface elevations for each array configuration are portrayed in Fig. 13 - 16 and include model runs with a C_T value of 0.5. The model results demonstrated that the water surface elevations were affected by energy extraction, with a reduction in tidal range upstream of the array being noted. The changes in water level were similar within (S1) and outside (S2) of the turbine farm domain (Fig. 13 and 14).
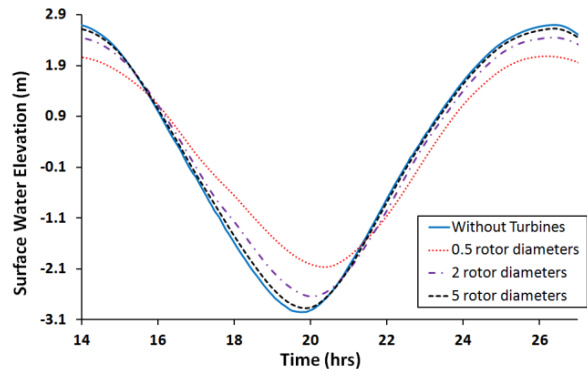

Figure 13: Comparison of surface water elevations inside turbine farm (S1) for the various array configurations
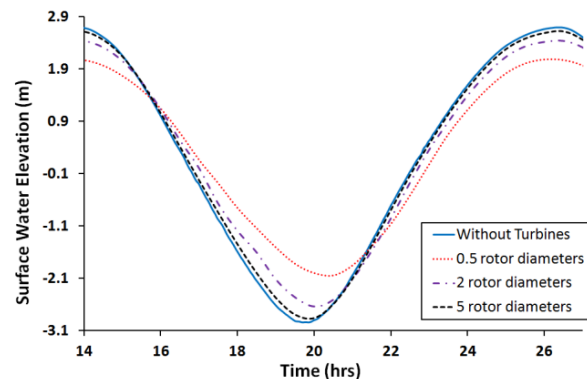

Figure 14: Comparison of surface water elevations outside turbine farm (S2) for the various array configurations

Similar effects on the tidal regime are observed both inside and outside of the turbine farm at the 3 simulated turbine densities (Fig. 13 and 14). There is a reduction in the tidal range at both locations and a time lag is yet again observed. The magnitude & extent of observed impacts were most significant at the highest turbine density and increasingly less significant at the lower densities.
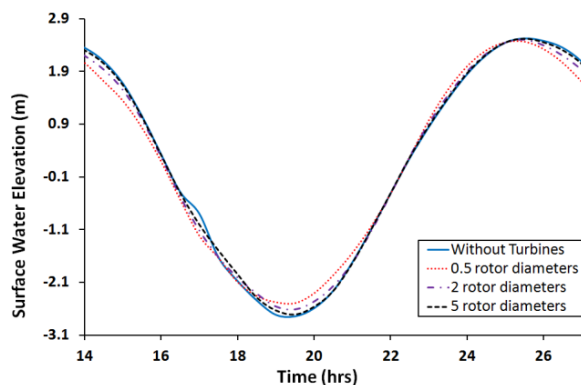
Figure 15: Comparison of surface water elevations downstream of turbine farm (D1) for the various array configurations
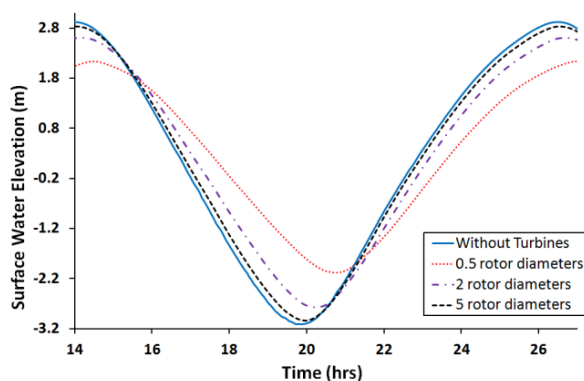

Figure 16: Comparison of surface water elevations upstream of turbine farm (U1) for the various array configurations

Downstream (D1), the high tide remains relatively unchanged because the open sea at the mouth dominates the flood tide which has not undergone extraction from the turbines (Fig. 15). The effect of energy extraction is still significant at low and high tides at the location downstream of the farm. At the upstream location (U1) at the highest turbine density, the effects of energy extraction impacts on the tidal range with an observed reduction in high tide level and an increase in low tide level (Fig. 16). Lower high tide levels upstream of the array have the potential to reduce the risk of flooding in the region. Energy extraction resulted in a heightening of low tide which means that some inter-tidal areas that are periodically wet and dry will now become permanently wet, and hence, impacts on the flora and fauna within the estuarine habitat.

The effect of energy extraction on the middle array density (2 rotor diameters) is less significant than that of the higher array density. The impacts are similar to the higher density but at a reduced magnitude.

At the lowest turbine density (Fig. 15 and 16) the impacts of energy extraction are much less significant; however, there is still a lowering of the high tide level and a heightening of the low tide level. Therefore, this is considered to be the most optimum turbine density of the 3 arrays simulated since this configuration minimises the hydro-environmental impacts and maximises power output.

5. Conclusions

This research involved the application of a modified 2D hydrodynamic model (DIVAST) to the Shannon Estuary, to quantify the effects of array configuration on the Hydro-environmental impacts of Tidal Turbines. The model was amended to account for the axial thrust induced by a tidal turbine and this parameter was included in the modified governing momentum equation. This modification was included as a sink term within the adjusted model, which was subsequently run to examine the hydro-environmental impacts and power extraction for three separate tidal turbine array densities. These array configurations were examined for a rotor diameter of 16 m with turbine spacings of 0.5, 2 and 5 rotor diameters.

The model results demonstrated that energy extraction would cause flow attenuation on the tidal currents downstream, upstream and within the array, while the velocities accelerated around the array because of flow obstruction due to 'blockage' effects. Increased sedimentation rates would be a consequential hydro-environmental impact from attenuation of water current, while flow acceleration would be responsible for increased erosion which would lead to an increase in suspended sediments. Consequently, this may impact on the estuarine habitat due to the increased sediment which would inevitably settle out of the water to cover inter-tidal flora. As a result, this would directly impact fauna which may rely on the flora as a primary food source. In addition, some species of marine mammals and fish might not be comfortable with the increased velocities associated with the flow diversion around the tidal farm. There is the potential that species migration could occur, or alternatively, they could move into the slower moving water within the tidal farm which may perhaps increase their risk of harm.

A time lag also occurs when energy extraction is considered, this delay manifests itself due to the flow being impeded when trying to pass through the turbines and as a result the water is held back which gives rise to a delay in the tide reaching high and low water. Surface water elevations are also affected with a reduction in tidal range upstream, within and outside of the turbine array field. The effect of energy extraction is responsible for lower high tide levels which would reduce the risk of flooding and higher low tide levels which would reduce the extent of inter-tidal mudflats. Another potential impact concerning the reduction of the high tide level in the estuary is that of navigational limitations such as a ship's draft which would subsequently reduce as the tidal range decreases. The scale and extent of the environmental impacts are larger for the smallest turbine array density, but were still significant for the larger densities. The surface water

elevations at high and low water reduce upstream of the estuary when the tidal stream turbines were included.

Acknowledgements

References

[1] Fraenkel, PL. (2007). Marine current turbines: pioneering the development of marine kinetic energy converters. P Mech Eng A-J Pow 2007;221:159e69.

[2] OpenHydro Press Release, OpenHydro successfully deploys 1MW commercial tidal turbine in the Bay of Fundy, in, 2009.

[3] Myers, L. E. and A. S. Bahaj (2012). "An experimental investigation simulating flow effects in first generation marine current energy converter arrays." Renewable Energy 37(1): 28-36.

[4] Falconer R.A., 1984. A mathematical model study of the flushing characteristics of a shallow tidal bay. In: Proceedings of the Institution of Civil Engineers, Part 2, Research and Theory, vol. 77(3), pp. 311 e332.

[5] Lin, B., Falconer, R.A ., 1997. Tidal flow and transport modelling using the Ultimate Quickest scheme. Journal of Hydraulic Engineering, ASCE 123 (4), 303e314.

[6] Hartnett, M., Nash, S., 2004. Modelling nutrients and chlorophyll-a dynamics in an Irish brackish waterbody. Environmental Modelling and Software 19 (1), 47 e56.

[7] Gao, G., Falconer, R.A., Lin, B., 2011. Numerical modelling of sediment-bacteria interaction processes in surface waters. Water Research 45 (5), 1951 e1960.

[8] Falconer, R.A., et al., (2001). DIVAST reference manual, Environmental Water Management Research Centre, Cardiff University.

[9] Houlsby, G.T., Draper, S., Oldfield, M.L.G., 2008. Application of Linear momentum actuator disc theory to open channel flow (No. OUEL 2296/08). University of Oxford.

[10] Ahmadian, R., R. Falconer, et al. (2012). "Far-field modelling of the hydro-environmental impact of tidal stream turbines." Renewable Energy 38(1): 107-116.

[11] Bryden, I. G. and S. J. Couch (2006). "ME1--marine energy extraction: tidal resource analysis." Renewable Energy 31(2): 133-139.

[12] SEI (2004). "Tidal and current energy resources in Ireland". Dublin, Sustainable Energy Ireland.

[13] Fraenkel, PL. (2007). Marine current turbines: pioneering the development of marine

kinetic energy converters. P Mech Eng A-J Pow 2007;221:159e69.

[14] Ahmadian, R. and R. A. Falconer (2012). "Assessment of array shape of tidal stream turbines on hydro-environmental impacts and available power." Renewable Energy.

[15] Fraenkel, P. (2002). "Power from marine currents." Proceedings of the Institution of Mechanical Engineers, Part A: Journal of Power and Energy 216(1): 1-14.